

## Ga<sub>1-x</sub>Mn<sub>x</sub>As: A Frustrated Ferromagnet

Gergely Zaránd<sup>1,2,3</sup> and Boldizsár Jankó<sup>1,4</sup>

<sup>1</sup>Materials Science Division, Argonne National Laboratory, 9700 South Cass Avenue, Argonne, Illinois 60429

<sup>2</sup>Lyman Physics Laboratory, Harvard University, Cambridge, Massachusetts 02145

<sup>3</sup>Research Group of the Hungarian Academy of Sciences, Institute of Physics, Technical University Budapest, Budapest, H-1521, Hungary

<sup>4</sup>Department of Physics, University of Notre Dame, Notre Dame, Indiana 46617

(Received 14 November 2001; published 8 July 2002)

Starting from a microscopic description of the exchange interaction in Ga<sub>1-x</sub>Mn<sub>x</sub>As, we derive an effective Mn-Mn interaction. Because of the strong spin-orbit coupling in the valence band, this effective interaction is highly anisotropic and has a spatial structure somewhat similar to dipolar interactions. The corresponding ground state has a finite magnetization but is intrinsically *spin disordered* even at zero temperature, explaining many features of the experimental data. Our results are relevant for many magnetic semiconductors.

DOI: 10.1103/PhysRevLett.89.047201

PACS numbers: 75.40.Gb, 75.30.Ds, 75.50.Dd

Semiconductors resisted for decades the concentrated efforts of a large community of researchers who wished to turn them into magnets. The benefits would be far reaching: spin could eventually be used to carry information in electronic devices. Unfortunately, any conventional method to produce semiconductor-magnet alloys failed repeatedly: magnetic materials were insoluble in most semiconductors. Not long ago [1], several classes of semiconductor materials finally gave in to a most powerful weapon against insolubility: the molecular-beam epitaxy machine. In Ga<sub>1-x</sub>Mn<sub>x</sub>As, for example, ferromagnetic transition temperatures as high as  $T_c \sim 110$  K have been reported [2]. Here we demonstrate that the victory above the natural tendency of the semiconductor not to mix with magnetic materials came with a considerable price: The strong spin-orbit interaction present in these materials together with spatial disorder results in *highly frustrated* magnetic correlations that remain in these systems down to the lowest temperatures. We find that magnetic semiconductors are most likely not ordinary ferromagnets, but that the intrinsic frustration pushes these systems into the regime of strongly spin disordered ferromagnets which also exhibit several features reminiscent of spin glasses and spin ice compounds [3,4].

Here we discuss in detail the important case of Ga<sub>1-x</sub>Mn<sub>x</sub>As. However, our results qualitatively apply to all magnetically doped II-VI and III-V compounds (and in general to any material with magnetic impurities) that show strong valence band spin-orbit interaction.

GaAs is a direct gap semiconductor with a valence band maximum at the center of the first Brillouin zone called  $\Gamma$  point [5]. The top of the valence band is formed by two twofold degenerate bands of  $p$  character. These two bands are degenerate in  $\Gamma$ . The orbitals involved in these bands form here a four-dimensional  $\Gamma_8$  irreducible representation. This fourfold degeneracy is due to the strong spin-orbit interaction that couples the  $l = 1$  angular momentum of the  $p$  orbitals to the electron spin ( $s = 1/2$ ), thereby

producing an effective total spin  $J = l + s = 3/2$  for the valence holes. Since the third  $p$  band with  $J = l - s = 1/2$  is separated from the two by a large spin-orbit splitting,  $\Delta_{so} \approx 340$  meV, for small hole concentrations it is reasonable to describe the valence band in terms of a two-band model [5,6]:

$$H_0 = \gamma_1 \frac{p^2}{2m} - \frac{1}{m} \left( \gamma_2 \sum_{\alpha} J_{\alpha\alpha} p_{\alpha\alpha} + \gamma_3 \sum_{\alpha \neq \beta} J_{\alpha\beta} p_{\alpha\beta} \right), \quad (1)$$

where  $m$  is the electron mass and the  $\gamma_i$ 's are the so-called Luttinger parameters [5]. The tensor operators  $J_{\alpha\beta}$  and  $p_{\alpha\beta}$  ( $\alpha, \beta = x, y, z$ ) are defined as  $Q_{\alpha\beta} = \frac{1}{2}(Q_{\alpha}Q_{\beta} + Q_{\beta}Q_{\alpha}) - \frac{1}{3}\delta_{\alpha\beta}\text{Tr}\{Q_{\alpha\beta}\}$ , with  $Q = p$  and  $J$ , referring to the momentum of the electrons and their  $J = 3/2$  effective spin. In the above equation the last two terms, proportional to  $\gamma_2$  and  $\gamma_3$ , describe the coupling between the effective spin of the valence hole and its orbital motion due to spin-orbit interaction. These terms will lift the fourfold degeneracy for nonzero momenta.

In Ga<sub>1-x</sub>Mn<sub>x</sub>As the Mn ion is believed to be in the Mn<sup>2+</sup> configuration, corresponding to a half-filled  $d$  shell with a total spin  $S = 5/2$  [7]. The general form of the interaction between the  $S = 5/2$  Mn spin and the  $J = 3/2$ -pseudospin holes depends on the momentum  $\mathbf{k}$  and  $\mathbf{k}'$  of the incoming and outgoing holes. However, close to the  $\Gamma$  point this momentum dependence is weak and we can approximate the coupling constants by their  $\mathbf{k}, \mathbf{k}' \rightarrow 0$  value at the  $\Gamma$  point. Thus the dominant part of the interaction has the following simple form [8]:

$$H_{\text{int}}(\mathbf{R}) = G\mathbf{S} \cdot \mathbf{J}(\mathbf{R}) \quad (2)$$

with  $G$  the exchange coupling, and  $\mathbf{J}(\mathbf{R})$  the spin density of the holes at the position  $\mathbf{R}$  of the Mn ion. Notice that  $J$  in Eq. (2) denotes the *total*  $J = 3/2$  spin of the valence holes. The above interaction Hamiltonian can be constructed based on a microscopic Anderson-type [9]

crystal field model but can also be established using purely symmetry considerations.

Equations (1) and (2) constitute the fundamental equations that describe the intricate interplay between the spin-orbit interaction in the valence band and the local moments. Although the model above can be refined to incorporate the third valence band, it already captures the most important features necessary to understand the properties of the ferromagnetic state and related phenomena in magnetic semiconductors. One of the key differences between this and most earlier calculations [10–12] is that we now take into account *both* the spin 3/2 character of the valence holes and the spatial disorder of the magnetic impurities [13]. Without this, one obtains an almost perfectly aligned ferromagnetic state [12].

In order to analyze the physical content of Eqs. (2) and (1) we first determine the effective interaction between two Mn ions at positions  $\mathbf{R}_1$  and  $\mathbf{R}_2$ , following the Ruderman-Kittel-Kasuda-Yoshida (RKKY) procedure [14]. Strictly speaking, in  $\text{Ga}_{1-x}\text{Mn}_x\text{As}$  the exchange interaction may be large enough to strongly polarize the valence band at low temperatures, thereby rendering the RKKY approximation inappropriate. However, we expect that it qualitatively captures already most important effects of the spin-orbit interaction. While the procedure itself is quite straightforward, an explicit evaluation of a more general type of interaction deduced in this way is extremely difficult even numerically. Fortunately, for the case of GaAs host one can make substantial progress by analytical calculations, provided that we rewrite Eq. (1) as

$$H_0 = \frac{\gamma_1}{2m} \left( p^2 - \nu \sum_{\alpha,\beta} J_{\alpha\beta} p_{\alpha\beta} + \delta H^{(4)} \right). \quad (3)$$

The first two parts of the Hamiltonian are rotationally invariant,  $\nu = (6\gamma_3 + 4\gamma_2)/5\gamma_1 \approx 0.77$ , and the octupolar term  $H^{(4)}$  can be shown to represent only a small correction [15]. Therefore, in leading order we can set  $\delta = 0$  and consider only the first two, spherically symmetric terms in Eq. (3), which we will denote as  $H_{\text{sp}}$ .

To diagonalize  $H_{\text{sp}}$  we choose the spin quantization axis to be in the  $\hat{z}$  direction. In this basis the energy of plane waves propagating along the  $\hat{z}$  direction is  $\epsilon_{\mu}(k = k_z) = k^2/2m_{\mu}$  with  $m_{\mu} = m_h = m/\gamma_1(1 - \nu) \approx 0.5m$  and  $m_{\mu} = m_l = m/\gamma_1(1 + \nu) \approx 0.07m$  the heavy and light hole masses for  $\mu = \pm 3/2$  and  $\pm 1/2$ , respectively. Eigenstates of  $H_{\text{sp}}$  propagating in other directions can then be constructed by simple rotations and are *chiral* in nature: The spin of the heavy holes is quantized along their propagation direction  $\hat{\mathbf{k}}$  and takes the values  $\mathbf{J} \cdot \hat{\mathbf{k}} = \pm 3/2$ . In this new chiral basis  $H_{\text{sp}}$  is given by the following simple form:

$$H_{\text{sp}} = \sum_{\mathbf{k},\mu} \frac{k^2}{2m_{\mu}} c_{\mathbf{k},\mu}^{\dagger} c_{\mathbf{k},\mu}, \quad (4)$$

where  $c_{\mathbf{k},\mu}^{\dagger}$  denotes the creation operator of a hole. The unperturbed ground state  $|0\rangle$  consists of two Fermi spheres.

The sphere with the larger radius contains heavy holes and includes about 90% of the valence band holes, while a sphere with the shorter radius is generated by the light holes. The price for diagonalizing  $H_{\text{sp}}$  is that the exchange coupling in the new basis becomes strongly momentum dependent:

$$H_{\text{int}}(\mathbf{R}) = \frac{G}{V} \sum_{\mathbf{k},\mathbf{k}'} \sum_{\alpha} S^{\alpha} c_{\mathbf{k}}^{\dagger} J^{\alpha}(\hat{\mathbf{k}}, \hat{\mathbf{k}}') c_{\mathbf{k}'} e^{-i(\mathbf{k}-\mathbf{k}')\mathbf{R}}. \quad (5)$$

Here  $J^{\alpha}(\hat{\mathbf{k}}, \hat{\mathbf{k}}')$  denotes the operator  $J^{\alpha}(\hat{\mathbf{k}}, \hat{\mathbf{k}}') \equiv D^{\dagger}(\hat{\mathbf{k}}) J^{\alpha} D(\hat{\mathbf{k}}')$ ,  $D(\hat{\mathbf{k}})$  is the spin 3/2 rotation matrix, and  $V$  the total volume of the sample. It is precisely this  $\hat{\mathbf{k}}$  dependence that generates the delicate magnetic properties of  $\text{Ga}_{1-x}\text{Mn}_x\text{As}$ . The spherical symmetry of  $H_{\text{sp}}$  implies that the interaction between two impurity spins  $S_1$  and  $S_2$  at a distance  $R = |\mathbf{R}_1 - \mathbf{R}_2|$  is given by

$$H_{\text{eff}} = -K_{\text{par}}(R) \mathbf{S}_1^{\parallel} \cdot \mathbf{S}_2^{\parallel} - K_{\text{perp}}(R) \mathbf{S}_1^{\perp} \cdot \mathbf{S}_2^{\perp}, \quad (6)$$

where  $\mathbf{S}^{\parallel}$  and  $\mathbf{S}^{\perp}$  denote the spin components parallel and perpendicular to  $\mathbf{R}_1 - \mathbf{R}_2$ . The form of  $H_{\text{eff}}$  is somewhat similar to that of dipolar interactions as it shows explicit dependence on the relative position of the Mn impurities. Indeed, the interaction between two Mn ions far away from each other is in large part mediated by holes propagating along the axis  $\mathbf{R}$  that connects them. Since the majority of the holes are heavy and their spin is quantized along the propagation direction, it immediately follows that the interaction must be different for spin components parallel and perpendicular to  $\mathbf{R}$ .

It turns out that the structure of the effective interaction Eq. (6) can be calculated analytically, although the details are rather technical and will be reported elsewhere [16]. The dominant part of the interaction comes from the heavy hole sector, since this has a much larger density of states at the Fermi level than the light hole band. The heavy hole contribution to  $K_{\text{par}}$  and  $K_{\text{perp}}$  can be expressed as

$$K_{\text{par/perp}}^{(\text{heavy})}(R) = 2\pi \epsilon_F g_h^2 C_{\text{par/perp}}^{(\text{heavy})}(k_{F,h}R), \quad (7)$$

where  $g_h = G\varrho_h$  is the dimensionless heavy-hole exchange coupling,  $\varrho_h$  is the heavy-hole density of states at the Fermi energy  $\epsilon_F$ , and  $k_{F,h}$  denotes the heavy hole Fermi momentum. The dimensionless functions  $C_{\text{par/perp}}(y)$  are clearly different (see Fig. 1), and in the  $y \rightarrow 0$  limit are approximately given by  $C_{\text{perp}}(y) \approx 1/y$  and  $C_{\text{par}}(y) \approx 1/2y$ . The contributions of the heavy-hole–light-hole and light-hole–light-hole sectors are given by similar scaling expressions and are proportional to  $g_h g_l$  and  $g_l^2$ , where  $g_l = G\varrho_l \approx 0.1g_h$  is the dimensionless coupling to the light holes and  $\varrho_l$  is light hole density of states at  $E_F$ .

In  $\text{Ga}_{1-x}\text{Mn}_x\text{As}$  only a small fraction  $f$  of the Mn ions gives a hole into the valence band. Although the exact value of this fraction is not precisely known, the latest experiments suggest [17] that for  $x = 0.05$  Mn concentration (corresponding to the highest  $T_c$ ) this fraction is about

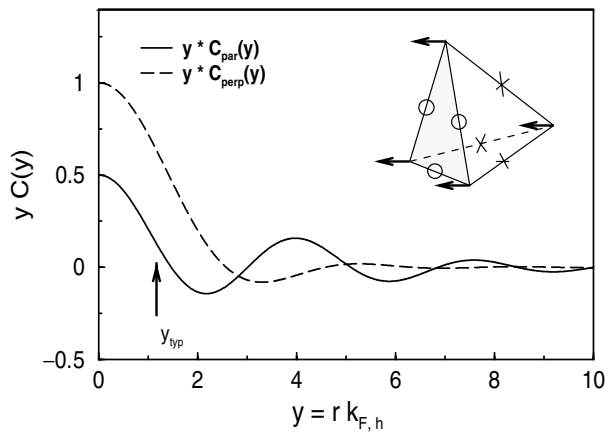


FIG. 1. Main figure: Spatial dependence of the two interaction parameters  $C_{\text{perp}}$  and  $C_{\text{par}}$  of Eq. (7). Only the contribution of the heavy hole sector is shown. The arrow indicates the typical value of  $y$  for  $x \approx 0.05$  and  $f \approx 0.25$ . Inset: Two Mn impurities close to each other tend to be aligned *perpendicular* to the axis connecting them. If we satisfy the bonds marked by circles, the other bonds with crosses remain unsatisfied, resulting in orientational frustration.

$f = 0.2-0.3$  (or  $k_{F,h} \approx 0.141/\text{\AA}$ ) and a typical Mn-Mn distance is approximately  $d_{\text{Mn-Mn}} \approx 12 \text{\AA}$ . Thus, for typical nearest-neighbor Mn ions  $K_{\text{perp}}$  is larger than  $K_{\text{par}}$  and *ferromagnetic*. However, this ferromagnetic interaction is *strongly anisotropic* as it tries to align a nearby pair of Mn spins parallel to the axis connecting them (see the illustration in Fig. 1). Since it is clearly impossible to simultaneously satisfy each pair of spins, this effect induces *orientational frustration* and influences the magnetic properties of  $\text{Ga}_{1-x}\text{Mn}_x\text{As}$  in a fundamental way. We investigated the implications of the anisotropy [18] on the magnetic properties of  $\text{Ga}_{1-x}\text{Mn}_x\text{As}$  by performing classical Monte Carlo simulations using the effective interaction of Eq. (6). In the simulations the Mn spins were replaced by classical angular variables,  $\mathbf{S} \rightarrow S\mathbf{\Omega}$ . The Mn ions were randomly distributed on a  $L \times L \times L$  face-centered cubic lattice with a probability  $x = 0.05$ . To take into account the finite mean free path  $l \approx 7 \text{\AA}$  of the valence holes, we used an exponential cutoff for the RKKY interaction [19]:  $K_{\text{par/perp}}(R) \rightarrow K_{\text{par/perp}}(R)e^{-R/l}$ .

In the inset of Fig. 2 we show the magnetization  $M \equiv \langle |\Omega_i| \rangle$  as a function of temperature. A spontaneous magnetization develops at low temperatures. The transition between the paramagnetic and magnetic phases takes place rather smoothly, and then increases approximately linearly with decreasing temperature, qualitatively similar to many experiments [20,21]. Both properties are characteristic of strongly disordered magnets [10]. The spontaneous magnetization, however, tends to a value at  $T = 0$  that is much *smaller* than that of a fully polarized ferromagnet. This reduction is clearly due to orientational disorder originating in the anisotropy of the interaction, and has nothing to do with possible antiferromagnetic couplings due to the RKKY oscillations of the Mn-Mn interaction [22]. To

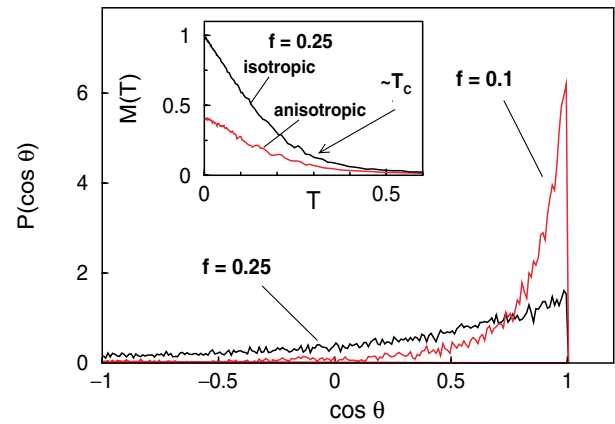


FIG. 2 (color online). Ground state probability distribution function of  $\cos\theta = \mathbf{\Omega} \cdot \mathbf{n}$  for a lattice with linear dimension  $L = 9 \times a$  ( $a = 5.65 \text{\AA}$ ) and  $x = 0.05$ . The unit vector  $\mathbf{n}$  gives the direction of the magnetization in the ground state. In the isotropic approximation, when  $K_{\text{par}} = K_{\text{perp}} = (2K_{\text{par}} + K_{\text{perp}})/3$ , the ground state is almost fully polarized, and thus  $P(\cos\theta) = \delta(\cos\theta - 1)$ . Inset: Magnetization as a function of temperature for these two cases. Temperature is measured in units of  $2\pi\epsilon_F g_h^2 S^2$ . For the isotropic interaction the magnetization saturates as  $T \rightarrow 0$ .

demonstrate this, we repeated the simulations by replacing the interaction in Eq. (6) by its angular average. The magnetization in this case *saturates* to its maximum value (see Fig. 2), and almost all Mn spins are fully polarized.

More information can be obtained about the ground state properties by measuring the distribution of  $\cos\theta \equiv \mathbf{\Omega}_i \cdot \mathbf{n}$ , where  $\mathbf{n}$  is the unit vector parallel to the ground state magnetization. Without the spatial anisotropy structure discussed here,  $P(\cos\theta) = \delta(\cos\theta - 1)$ , since the spins are fully aligned. As shown in Fig. 2, in the system with the correct exchange interaction, the quantity  $\cos\theta$  has a very broad but asymmetric distribution. Depending on the actual value of  $f$  the distribution has more or less weight in the vicinity of  $\cos\theta = 1$ : For  $f = 0.1$  the Mn spins tend to point approximately into the direction of the global magnetization; however, they deviate at the average by an angle  $\theta \sim 30^\circ$  and the magnetization is reduced considerably by  $\sim 20\%$ . The ground state becomes more spin disordered for larger carrier fractions: The distribution has less weight at  $\cos\theta = 1$  and many of the spins are aligned *antiferromagnetically* with respect to the global magnetization, thus reducing the magnetization by about  $\sim 50\%$ .

The large reduction in the magnetization we find here has been observed experimentally [20,23]. The non-mean-field-like shape of the  $M(T)$  curve is characteristic to unannealed and “overannealed” samples [21] with  $T_c < 80 \text{ K}$ , and the measured in-plane saturation magnetization of  $\text{Ga}_{1-x}\text{Mn}_x\text{As}$  is indeed about 50% less than the value that would correspond to the known Mn concentration. Cooling down these samples in a relatively weak external field ( $H \leq 4T \ll T_c$ ) results in a 20%–40% increase in the  $T = 0$  magnetization. Also, the broad linewidth of

ferromagnetic resonance data is consistent with the substantial intrinsic spin disorder we find [24].

The intrinsic spin disorder above could be the reason for various resistance anomalies. Since spin disorder produces a large spin scattering contribution to the resistivity, it may provide an explanation to the large negative magnetoresistance of  $\text{Ga}_{1-x}\text{Mn}_x\text{As}$  alloys with smaller  $T_c$  at temperatures  $T \ll T_c$ . It can also possibly explain why these materials exhibit a resistance peak *precisely* at the ferromagnetic phase transition: Because of the spin disorder present in the ground state, the magnetic order parameter which appears at  $T_c$  also involves “disordered” fluctuations corresponding to *finite* momenta. These finite momentum components of the soft modes may result in a maximum of the resistance at  $T_c$ . This should be contrasted to any conventional ferromagnet, which exhibits predominantly long wavelength soft modes and, therefore, shows no peak in the resistivity at  $T_c$  [25].

The results of our simulations are consistent with a highly spin disordered ferromagnetic ground state with spin-glass-like behavior. Indeed, we found many metastable, *macroscopically* different local energy minima of the Hamiltonian, extremely close to the ground state, a characteristic property of spin glass systems. The precise nature of the ground state can be determined experimentally. One of the typical experimental signatures of a spin glass state would be the history dependence of the high field magnetization in fields parallel to the film, or the difference between field cooled and zero field cooled susceptibilities. This is a straightforward experiment, which can be performed with already existing samples and apparatus. However, the outcome would provide a highly valuable insight into the true order present in these magnetically ordered semiconducting systems. Stronger evidence for spin glass behavior could be provided by nonlinear susceptibility or neutron scattering data [3].

The annealing experiments suggest that optimally annealed samples have a higher carrier concentration and the effects we discussed above are less pronounced: Their magnetization curve saturates more rapidly and tends to larger values, the ferromagnetic resonance (FMR) signal becomes narrower, and the resistivity anomaly at  $T_c$  also gets suppressed. For these samples  $E_F$  becomes comparable to  $\Delta_{so}$  and our four-band approach may be inappropriate.

We are grateful to Professor Peter B. Littlewood, Professor Allan H. MacDonald, Professor Peter Schiffer, and especially Professor Jacek K. Furdyna for stimulating discussions. This research has been supported by the U.S. DOE, Office of Science, the NSF Grants No. DMR-9985978 and No. DMR97-14725, and Hungarian Grants No. OTKA F030041, No. T038162, and No. N31769. G. Z. is an Eotvos Fellow.

- [1] J. K. Furdyna, J. Appl. Phys. **64**, R29 (1988).
- [2] H. Ohno, Science **281**, 951 (1998).
- [3] K. Binder and A. P. Young, Rev. Mod. Phys. **58**, 801 (1986).
- [4] J. Snyder *et al.*, Nature (London) **413**, 48 (2001).
- [5] J. S. Blakemore, J. Appl. Phys. **53**, R123 (1982).
- [6] W. Kohn and J. M. Luttinger, Phys. Rev. **98**, 915 (1955).
- [7] M. Linnarson, Phys. Rev. B **55**, 6938 (1997); J. Szczytko *et al.*, Phys. Rev. B **60**, 8304 (1999); J. Okabayashi *et al.*, Phys. Rev. B **58**, R4211 (1998).
- [8] P. Kacman, Semicond. Sci. and Technol. **16**, R25 (2001).
- [9] See D. L. Cox and A. Zawadowski, Adv. Phys. **47**, 599 (1998).
- [10] R. N. Bhatt and X. Wan, Int. J. Mod. Phys. C **10**, 1459 (1999); Mona Berciu and R. N. Bhatt, Phys. Rev. Lett. **87**, 107203 (2001).
- [11] J. König, H. H. Lin, and A. H. MacDonald, Phys. Rev. Lett. **84**, 5628 (2000).
- [12] For recent reviews see J. König *et al.*, in *Electronic Structure and Magnetism of Complex Materials*, edited by D. J. Singh and D. A. Papaconstantopoulos (Springer-Verlag, Berlin, 2002); T. Dietl, cond-mat/0201282.
- [13] Monte Carlo simulations taking both band structure effects and disorder into account have been performed on relatively small system sizes in a different regime by J. Schliemann *et al.*, Phys. Rev. B **64**, 165201 (2001).
- [14] K. Yosida, *Theory of Magnetism* (Springer-Verlag, Berlin, 1996).
- [15] A. Baldereschi and N. O. Lipari, Phys. Rev. B **8**, 2697 (1973).
- [16] G. Zarand and B. Janko (unpublished).
- [17] T. Dietl *et al.*, Science **287**, 1019 (2000).
- [18] We neglected the effect of *global* anisotropy energy terms, which determine the actual orientation of the macroscopic magnetization in the symmetry broken phase. They are about 1% of the average exchange interaction energy between neighboring spins, and therefore do not influence the microscopic structure discussed here.
- [19] H. Ohno *et al.*, Phys. Rev. Lett. **68**, 2664 (1992).
- [20] A. VanEsch *et al.*, Phys. Rev. B **56**, 13 103 (1997).
- [21] S. J. Potashnik *et al.*, Appl. Phys. Lett. **19**, 1495 (2001).
- [22] A very weak noncollinearity has been inferred recently even from the spin-wave spectrum of a model with no spin-orbit interaction by J. Schliemann and A. H. MacDonald, Phys. Rev. Lett. **88**, 137201 (2002).
- [23] H. Ohno and F. Matsukura, Solid State Commun. **117**, 179 (2001).
- [24] J. K. Furdyna *et al.* (unpublished).
- [25] P. Majumdar and P. B. Littlewood, Nature (London) **395**, 479 (1998). This work also suggested spin polaronic contributions as the explanation of the resistance maximum. However, this scenario predicts a maximum *above*  $T_c$  (in contrast to the observed maximum at  $T_c$ ). Also, according to M. J. Calderon, L. Brey, and P. B. Littlewood, Phys. Rev. B **62**, 3368 (2000), the temperature range where these polaronic excitations exist in  $\text{Ga}_{1-x}\text{Mn}_x\text{As}$  is probably rather limited.